Boundary-induced spin-density waves in linear Heisenberg antiferromagnetic spin chains with $S \geqslant 1$

Dayasindhu Dey,[1,*] Manoranjan Kumar,[1,†] and Zoltán G. Soos[2,‡]
[1]*S. N. Bose National Centre for Basic Sciences, Block JD, Sector III, Salt Lake, Kolkata 700098, India*
[2]*Department of Chemistry, Princeton University, Princeton, New Jersey 08544, USA*
(Received 24 June 2016; revised manuscript received 1 September 2016; published 14 October 2016)

Linear Heisenberg antiferromagnets (HAFs) are chains of spin-S sites with isotropic exchange J between neighbors. Open and periodic boundary conditions return the same ground-state energy per site in the thermodynamic limit, but not the same spin S_G when $S \geqslant 1$. The ground state of open chains of N spins has $S_G = 0$ or S, respectively, for even or odd N. Density-matrix renormalization-group calculations with different algorithms for even and odd N are presented up to $N = 500$ for the energy and spin densities $\rho(r,N)$ of edge states in HAFs with $S = 1$, $3/2$, and 2. The edge states are boundary-induced spin density waves (BI-SDWs) with $\rho(r,N) \propto (-1)^{r-1}$ for $r = 1,2,\ldots,N$. The SDWs are in phase when N is odd, are out of phase when N is even, and have finite excitation energy $\Gamma(N)$ that decreases exponentially with N for integer S and faster than $1/N$ for half integer S. The spin densities and excitation energy are quantitatively modeled for integer S chains longer than 5ξ spins by two parameters, the correlation length ξ and the SDW amplitude, with $\xi = 6.048$ for $S = 1$ and 49.0 for $S = 2$. The BI-SDWs of $S = 3/2$ chains are not localized and are qualitatively different for even and odd N. Exchange between the ends for odd N is mediated by a delocalized effective spin in the middle that increases $|\Gamma(N)|$ and weakens the size dependence. The nonlinear sigma model (NLσM) has been applied to the HAFs, primarily to $S = 1$ with even N, to discuss spin densities and exchange between localized states at the ends as $\Gamma(N) \propto (-1)^N \exp(-N/\xi)$. $S = 1$ chains with odd N are fully consistent with the NLσM; $S = 2$ chains have two gaps $\Gamma(N)$ with the same ξ as predicted whose ratio is 3.45 rather than 3; the NLσM is more approximate for $S = 3/2$ chains with even N and is modified for exchange between ends for odd N.

DOI: 10.1103/PhysRevB.94.144417

I. INTRODUCTION

The Hilbert space of a system of N spins S has dimension $(2S+1)^N$. The total spin $S_T \leqslant NS$ and its z components are conserved for isotropic (Heisenberg) exchange interactions between spins. The simplest case is a chain with equal exchange J between nearest neighbors. A great many theoretical and experimental studies have been performed on the linear Heisenberg antiferromagnet (HAF), Eq. (1) below, with $S = 1/2$ and $J > 0$. There are multiple reasons why. First, there are good physical realizations of spin-1/2 chains in inorganic crystals with localized spins on metal ions and in organic crystals based on one-dimensional (1D) stacks of radical ions. Second, the Hilbert space is smallest for $S = 1/2$ for any choice of exchange interactions, small enough to access the full spectrum and thermal physics for comparison with experiment. Third, long ago Bethe and Hulthén obtained the exact ground state (GS) [1] of the infinite chain with antiferromagnetic exchange between nearest neighbors, a prototypical gapless many-body system with quasi-long-range order.

HAFs and related chains with $S \geqslant 1$ came to the fore with Haldane's conjecture based on field theory that integer S chains are gapped [2]. Shortly thereafter, White introduced the density-matrix renormalization-group (DMRG) method that made possible accurate numerical calculation of the ground-state properties of $S \geqslant 1$ chains [3]. The thermodynamic limit of spin chains with exchange interactions leads to quantum phase diagrams with many interesting correlated phases. According to the valence bond solid (VBS) analysis [4], integer S chains have localized edge states with spin $s = S/2$. DMRG studies of finite chains have confirmed edge states in both integer [5,6] S and half integer [7,8] S chains. Machens *et al.* [9], have recently discussed short $S \geqslant 1$ HAFs with comparable energies for bulk excitations and edge states. They summarize previous studies such as the relation of $S \geqslant 1$ HAFs to the nonlinear σ model (NLσM), its application to edge states, the VBS model, and its valence bond diagrams. Qin *et al.* [7], applied DMRG to HAFs up to 100 spins to discuss the energies of edge states and to distinguish between chains of integer and half integer S. DMRG is quantitative for $S = 1$ HAFs of $N \leqslant 100$ spins with correlation length $\xi \sim 6$ and large Haldane gap. Longer chains are necessary for the $S = 2$ HAF with $\xi \sim 50$ or for the gapless $S = 3/2$ HAF.

In this paper we consider edge states of HAFs with $S = 1$, $3/2$, and 2 in systems of up to 500 spins. We use conventional DMRG for chains with an even number of spins and another algorithm for chains with an odd number of spins. We compute and model the spin densities of edge states as well as their excitation energies. The Hamiltonian of the spin-S HAF chain with open boundary conditions (OBCs) is

$$H_S(N) = J \sum_{r=1}^{N-1} \vec{S}_r \cdot \vec{S}_{r+1}. \tag{1}$$

The spin at site r is S_r, the total spin S_T and its z component S^z are conserved, and $J = 1$ is a convenient unit of energy.

The terminal spins $r = 1$ and N are coupled to only one spin in Eq. (1). Periodic boundary conditions (PBCs) also have J between sites 1 and N. Every spin is then coupled to

*dayasindhu.dey@bose.res.in
†manoranjan.kumar@bose.res.in
‡soos@princeton.edu

two neighbors, the system has translational symmetry, and the smallest S_T is expected in the ground state for AF exchange. Indeed, the GS of PBC chains is a singlet, spin $S_G = 0$, except for odd N and half integer S, when $S_G = 1/2$. The sectors of integer and half integer S are disjoint, and even N is conventionally taken for the thermodynamic limit. As noted by Faddeev and Takhtajan, the thermodynamic limit of the $S = 1/2$ HAF with odd N is not well understood [10].

HAFs with OBCs are fundamentally different because there is no energy penalty for parallel spins at sites 1 and N. The GS of Eq. (1) remains a singlet for even N, but it becomes a multiplet with $S_G = S$ and Zeeman degeneracy $(2S_G + 1)$ for odd N. The lowest-energy triplet is necessarily an excited state when N is even. For integer S, the singlet is an excited state when N is odd, while for half integer $S > 1/2$ the doublet is an excited state when N is odd. Except in the $S = 1/2$ case, S_G depends on the boundary conditions for arbitrarily large systems. It follows that HAFs with OBCs support edge states with $S_G \geqslant 1$ whose energies per site become degenerate in the thermodynamic limit with those of PBC systems with $S_G = 0$ or 1/2.

We define the energy gaps of edge states in chains of N spins as

$$\Gamma_S(N) = E_0(S,N) - E_0(0,N), \tag{2}$$

where $E_0(S,N)$ is the lowest energy in the sector with total spin S. Even N leads to $\Gamma_S(N) > 0$. Odd N leads to $\Gamma_S(N) < 0$ for integer S and to $\Gamma_S(N) < 0$ relative to $E_0(1/2,N)$ for half integer S. Since DMRG algorithms conserve S^z rather than S, the most accurate results are the GS in sectors with increasing S^z and $\Gamma_S(N) > 0$. Otherwise, the singlet or doublet is an excited state in the $S^z = 0$ sector for integer S or in the $S^z = 1/2$ sector for half integer S. The size dependence of $\Gamma_S(N)$ is faster than $1/N$, which distinguishes gap states from bulk excitations that may also have zero gap in the thermodynamic limit.

We shall characterize edge states using spin densities and call them boundary-induced spin density waves (BI-SDWs). A BI-SDW is more descriptive than an edge state and is more accurate than a localized state, since BI-SDWs are not localized in half integer S chains. By convention, we choose the Zeeman level $S^z = S$ when $S \geqslant 1$ and define the spin density at site r as

$$\rho(r,N) = \langle S^z_r \rangle, \quad r = 1,2 \ldots N. \tag{3}$$

The expectation value is with respect to the state of interest. Singlet states have $\rho(r,N) = 0$ at all sites. SDWs with $S \geqslant 1$ have equal spin density at r and $N + 1 - r$ by symmetry in chains, $\rho(N) = \rho(1) > 0$ by construction and $\rho(r,N) \propto (-1)^{r-1}$. It is advantageous to focus on spin densities rather than energy gaps. Spin densities are exclusively associated with $S > 0$ states while the $\Gamma_S(N)$ in Eq. (2) are small differences between extensive energies.

The NLσM is a good approximation for $S \geqslant 1$ HAFs, and theoretical discussions have focused as much on field theory as on spin chains [11–13]. The model for integer S chains relates edge states to an effective Hamiltonian between spins $s' = S/2$ at the ends [9]:

$$H_{\rm eff}(N) = (-1)^N J_e \exp(-N/\xi) \vec{s'}_1 \cdot \vec{s'}_N. \tag{4}$$

The correlation length ξ and exchange J_e are fit to DMRG results for H_S. An interesting point is that ξ refers to the bulk, the singlet GS in the thermodynamic limit, as has been confirmed within numerical accuracy in $S = 1$ chains [5]. The $S = 2$ chain has two gap states that afford more stringent tests of Eq. (4). For example, the ratio of the two gaps is necessarily 3:1 for $s'_1 = s'_N = 1$. Edge states in HAFs with half integer $S \geqslant 3/2$ have been discussed [7,9,14] using $H_{\rm eff}$ with effective spins $s' = (S - 1/2)/2$ and effective exchange $J'(N)$ that decreases faster than $1/N$ but not exponentially.

Our principal goal is the quantitative description of edge states in HAFs that are sufficiently long to neglect bulk excitations in $S = 3/2$ or 2 chains. The paper is organized as follows. Section II summarizes the conventional DMRG algorithm for even N and a different algorithm for odd N that is related to Y junctions. Section III presents boundary induced spin densities and gaps for $S = 1$ and 2 chains with finite Haldane gaps and finite correlation lengths ξ. DMRG returns $\xi = 6.048$ for $S = 1$ chains, in agreement with 6.03(1) reported previously [5], and $\xi = 49.0$ for $S = 2$ chains. DMRG spin densities are fit quantitatively by BI-SDWs that are in phase for odd N and out of phase for even N. The coupling $H_{\rm eff}(N)$ between ends is quantitative for $S = 1$ chains and is semiquantitative for $S = 2$ chains, in qualitative agreement with the VBS picture of localized spins. Section IV presents the BI-SDWs and gaps of the $S = 3/2$ chain. The BI-SDWs are not localized in this case. The singlet-triplet gap $\Gamma_1(N)$ for even N decreases faster than $1/N$, as anticipated by Ng [14]. The gap $\Gamma_{3/2}(N)$ for odd N requires a modified $H_{\rm eff}(N)$ with a delocalized spin in the central part in addition to spins at the ends. The delocalized spin rationalizes $|\Gamma_{3/2}(N)| > \Gamma_1(N)$ and a weaker size dependence. The Discussion section summarizes the limited nature of connections to the NLσM or to VBS.

II. DMRG ALGORITHMS

By now, DMRG is a mature numerical method for 1D systems [15,16]. It gives excellent low-energy properties and has been widely applied to spin chains. A conventional DMRG calculation starts with a superblock that consists of four sites: one site in the left block, one in the right block, and two new sites, the central sites. The left and right blocks increase by one site as two new sites are added at every step. The procedure generates a chain with OBCs and an even number of sites N. The vast majority of DMRG calculations has been performed on chains with even N. White has discussed [17] an algorithm with one rather than two central sites that speeds up the computational time by a factor of 2 to 4. The method was tested on an $S = 1$ HAF of 100 spins.

We use conventional DMRG for spin chains with even N and adapt an algorithm for odd N that was developed for Y junctions [18]. Y junctions of $N = 3n + 1$ spins have three arms of n spins plus a central site for which we recently presented an efficient DMRG algorithm. Figure 2 of [18] shows the growth of the infinite DMRG algorithm. A chain of $N = 2n + 1$ spins can be viewed as two arms of n spins plus a central site. The algorithm takes the system as an arm plus the central site and the environment as the other arm. Since the system of $n + 1$ spins at step n becomes the environment

TABLE I. Representative previous and present DMRG calculations for HAF chains with spin $S = 2$ or $3/2$ and $N \geqslant 100$ sites. The truncation error is $P(m)$ when m states are kept per block.

N, Ref.	S	m	$P(m)$
270 [6]	2	210	1×10^{-7}
150 [19]	2	250	1×10^{-6}
100 [7]	3/2	120	3×10^{-7}
192 [8]	3/2	500–800	1×10^{-7}–1×10^{-8}
400	2	600	1.1×10^{-7}
399	2	500	8.5×10^{-9}
400	3/2	460	8.4×10^{-7}
399	3/2	460	1.4×10^{-7}

at the next step, the chain grows by two spins at each step. The procedure described for Y junctions [18] holds with one fewer arm for chains of $N = 2n + 1$ spins.

The accuracy of the algorithm for odd N is comparable to conventional DMRG, as has already been shown for Y junctions [18]. In either algorithm, new sites are coupled to the most recently added sites and the superblock Hamiltonian contains only new and once renormalized operators. Table I has representative DMRG results for the ground states of $S = 2$ and $3/2$ chains with $N \geqslant 100$ spins. The index m is the number of states kept per block. The truncation error is $P(m) = 1 - \sum_j^m \omega_j$ where the sum is over the eigenvalues ω_j of the density matrix. Several sweeps of finite DMRG calculations are required for $S = 3/2$ or 2, with N calculations per sweep, and finite DMRG is necessary for accurate spin densities. Increasing m rapidly increases the required computer resources for long chains and involves tradeoffs. We have checked our results against previous studies in Table I as well as against $S = 1$ chains and find comparably small or smaller $P(m)$ that amount to evolutionary improvements for even N. The algorithm for odd N returns equally small $P(m)$.

In the following we have set m according to Table I and performed five to ten sweeps of finite DMRG for $S = 2$ and $3/2$ chains. We estimate that GS energies per site are accurate to 10^{-8} for $S = 1$ chains, to 10^{-6} for $S = 3/2$, and to 10^{-5} for $S = 2$. Comparable estimates are discussed using various criteria in works cited in Table I. The energy gaps $\Gamma_S(N)$ between the GS in sectors with different total spin are accurate to 10^{-5} for $S = 1$ and to 10^{-4} for $S = 3/2$ or 2. Haldane gaps $\Delta(S)$ have been reported [20] to $S = 5$, again using various criteria. We estimate that spin densities are accurate to better than 10^{-4} based, for example, on DMRG calculations with different algorithms for N and $N - 1$. Accurate $\rho(r,N)$ are readily obtained in large systems whose $\Gamma_S(N)$ are not accessible.

III. INTEGER SPIN, $S = 1$ AND 2

We start with the extensively studied $S = 1$ HAF with OBCs and even N. The large Haldane gap [5,20] $\Delta(1) = 0.4105$ reduces the computational effort. The singlet-triplet gap $\Gamma_1(N)$ in Eq. (2) decreases rapidly with system size. The GS alternates between $S_G = 0$ and 1 for even and odd N, respectively. We evaluate $\Gamma_1(N)$ for even N as the difference of the total energy in the sectors $S^z = 0$ and 1. In addition,

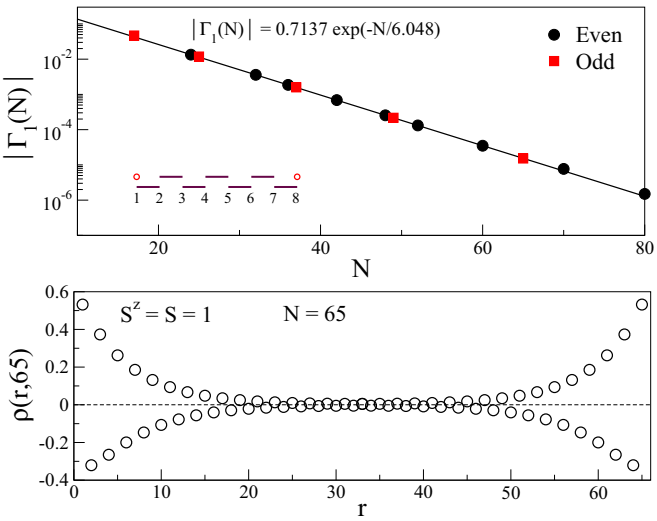

FIG. 1. Upper panel: Singlet-triplet gap $|\Gamma_1(N)|$ of $S = 1$ chains with N spins, even or odd, in Eq. (1). Inset: VBS valence bond diagram for $N = 8$. Lower panel: Spin densities $\rho(r,65)$ of the $S = 1$ chain with 65 spins.

we also obtain $\Gamma_1(N) < 0$ for odd N using the first excited state in the $S^z = 0$ sector. The excited state is accurate to 10^{-6} for $m > 300$. As shown in the upper panel of Fig. 1 with different symbols for even and odd N, $|\Gamma_1(N)|$ decreases as $J_e \exp(-N/\xi)$ with $\xi = 6.048$. The effective exchange between the ends is $J_e = 0.7137$ in Eq. (4) with spins $s' = 1/2$. The effective Hamiltonian is quantitative for $S = 1$ chains. The gap at $N = 80$ is 1.5×10^{-6}, which still exceeds the estimated numerical accuracy. The inset shows the relevant VBS valence bond diagram [4]. Each line is a singlet pair, $(\alpha\beta - \beta\alpha)/\sqrt{2}$, between $S = 1/2$ spins, two per $S = 1$ site, and the circles are unpaired spins at the ends.

Comparable DMRG accuracy for $S = 1$ chains with even N has been discussed previously. Sørensen and Affleck found $\xi = 6.07$ for $\Gamma_1(N)$ and 6.028(3) for spin densities [21]. White and Huse obtained [5] the GS energy per site very accurately and reported $\xi = 6.03(1)$ for the spin densities of a 60-site chain with an auxiliary spin-1/2 at one end [site $N + 1$ in Eq. (1)]. Schollwöck *et al.* [6] discussed the same procedure for $S = 2$ chains with even N and an auxiliary spin-1 at one end. Auxiliary spins at both ends with adjustable exchange to sites 1 and N can be used to study bulk excitations [5]. In this paper, we shall not resort to auxiliary spins. We always consider BI-SDWs at both ends of chains.

The spin densities $\rho(r,65)$ in Fig. 1, lower panel, are for the GS of the 65-spin chain. We take $S^z = 1$ and obtain positive $\rho(r)$ at odd numbered sites and negative $\rho(r)$ at even numbered sites, respectively. All chains with $S > 0$ have $\rho(r,N) \propto (-1)^{r-1}$, which is why we call them BI-SDWs. Table II lists the spin densities of the first ten sites in chains of 66/65 spins and 48/47 spins. The 66/65 spin densities clearly refer to the same triplet and speak to the numerical accuracy since different algorithms are used. The spin density at site 1 is slightly greater than 1/2, and so is the total spin density to odd-numbered sites. The total spin density to an even-numbered site approaches 1/2 from below and exceeds 0.45 at $r = 10$.

TABLE II. DMRG results for spin densities at the first ten sites of $S = 1$ chains of N spins.

Site	$N = 66$	$N = 65$	$N = 48$	$N = 47$
1	0.53204	0.53204	0.53198	0.53211
2	−0.32090	−0.32091	−0.32081	−0.32102
3	0.37324	0.37326	0.37311	0.37342
4	−0.26515	−0.26517	−0.26495	−0.26541
5	0.26242	0.26245	0.26216	0.26275
6	−0.19992	−0.19996	−0.19958	−0.20037
7	0.18544	0.18549	0.18502	0.18599
8	−0.14688	−0.14694	−0.14635	−0.14757
9	0.13166	0.13173	0.13101	0.13249
10	−0.10675	−0.10685	−0.10597	−0.10777

The apparent exponential decrease of $|\rho(r,N)|$ does not hold for the first few sites since, for example, $|\rho(2)| < \rho(3)$. The triplets are identical near the ends but of course differ at the middle of the chain, where $\rho(33,65) = 4.82 \times 10^{-3}$ becomes $\rho(33,66) = \rho(34,66) = 3.7 \times 10^{-4}$. Out-of-phase BI-SDWs for even N have small but equal ρ at sites $N/2$ and $N/2+1$. The 48/47 data illustrate the weak size dependence of spin densities at the ends. Well-defined edge states must become size independent. The first ten sites of $N = 65$ or 66 chains are close to the thermodynamic limit of BI-SDWs.

To minimize the even-odd variations of spin densities and to divide out an overall scale factor, we consider the function

$$f(r,N) = \frac{\rho(r-1) - \rho(r+1)}{\rho(r-1) + \rho(r+1)} \approx -\frac{\partial}{\partial r} \ln|\rho(r,N)|. \quad (5)$$

$f(r,N)$ is odd with respect to the chain's midpoint while $|\rho(r,N)|$ is even. Figure 2 shows $\ln|f(r,N)|$ for $S = 1$ chains up to the middle, $r \leqslant (N+1)/2$. The DMRG points near the edge become size independent. Except for the first few (~ 10) sites, $f(r,N)$ is constant up to about $N/2 - 2\xi$. The difference between even and odd N is clearly seen in the middle region, and $f(r,N)$ for even and odd pairs is a convenient way to present spin densities directly without making any assumptions about the appropriate model or interpretation. It follows that the thermodynamic limit is $\ln|f(r)| = -1.801$. The lines are fits as discussed below using the correlation length $\xi = 6.048$ from the gap $\Gamma_1(N)$, in accord with the NLσM's expectation of equal ξ for gaps and spin densities.

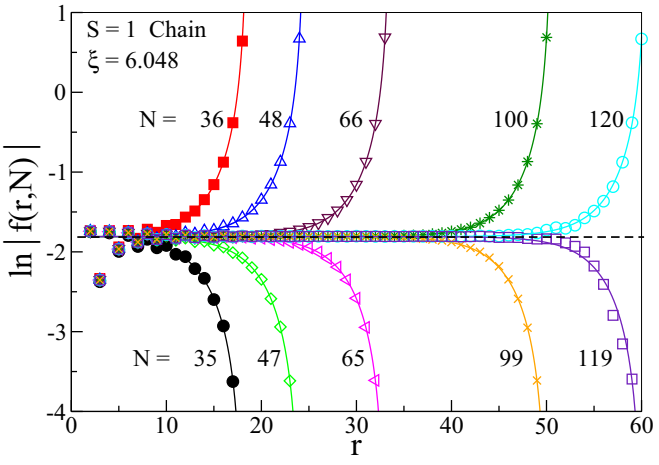

FIG. 2. Symbols are DMRG spin densities in $f(r,N)$, Eq. (5), to the middle of $S = 1$ chains of N spins. The lines are Eq. (8) with correlation length $\xi = 6.048$. The horizontal dashed line is the thermodynamic limit.

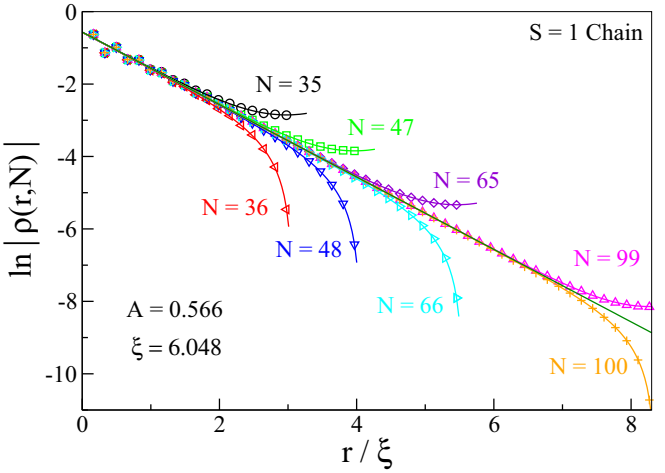

FIG. 3. Symbols are DMRG results for $|\rho(r,N)|$ to the middle of $S = 1$ chains. Lines are Eq. (7) with $\xi = 6.048$ and $A = 0.566$. Even and odd N deviate from $A\exp(-r/\xi)$ near the middle of chains.

The magnitudes of the spin densities are shown in Fig. 3 as a function of r/ξ up to the middle of the chains. They decrease as $A\exp(-r/\xi)$ and deviate upward in the middle for odd N, and downwards for even N. The amplitude A is independent of system size when $N/\xi > 5$.

To model the spin densities of integer S chains, we introduce SDWs at the left and right ends:

$$\rho(r,N) = A(-1)^{r-1}[\exp(-r/\xi) - (-1)^N \exp(-(N+1-r)/\xi)]. \quad (6)$$

The SDWs are in phase for odd N when all odd-numbered sites have $\rho > 0$; they are out of phase for even N with equal ρ at sites $N/2$ and $N/2+1$. Except for [21], the spin densities have been assumed to decrease exponentially, thereby ignoring contributions from the other end. While that is the case in the thermodynamic limit, $N > 10\xi$ is minimally required to neglect contributions from the other BI-SDW in the middle. Since the system size in DMRG calculations rarely exceeds 10ξ, it is advantageous to consider both ends. We have

$$\rho(r,N) = 2A(-1)^{r-1}\exp(-(N+1)/2\xi) \times \begin{cases} \cosh[(N+1-2r)/2\xi] & (\text{odd}N) \\ \sinh[(N+1-2r)/2\xi] & (\text{even}N) \end{cases}. \quad (7)$$

The postulated BI-SDWs lead to

$$f(r,N) = \tanh(1/\xi) \begin{cases} \tanh[(N+1-2r)/2\xi] & (\text{odd}N) \\ \coth[(N+1-2r)/2\xi] & (\text{even}N) \end{cases}. \quad (8)$$

The relative phase of the SDWs matters within $\pm 2\xi$ of the middle. The range of r is the same for N and $N-1$ when N is even.

The lines in Fig. 2 are $\ln|f(r,N)|$ for $\xi = 6.048$ and continuous r in Eq. (8). The thermodynamic limit is $f(r) = \tanh(1/\xi)$, the dashed line in Fig. 2, and it reduces to $1/\xi$ for an integer S chain with small Haldane gap and very long spin correlations. The continuum approximation for discrete chains is better for $S = 2$ than for $S = 1$ and is even better for larger S.

The correlation length ξ is accurately obtained using both even and odd chains. The $N = 119/120$ spin densities indicate a gap of $\Gamma_1(120) = 1.72 \times 10^{-9}$ that is far below the accuracy of the energy difference. DMRG spin densities are also limited, however, to less than 149/150; there the $\rho(r,N)$ show considerable scatter where $f(r,N)$ has even-odd variations. The SDW amplitude $A = 0.566$ in Fig. 3 accounts quantitatively for spin densities aside from the first few. The parameters ξ and A suffice for all fits in Figs. 2 and 3. Our results for $S = 1$ edge states extend the analysis to chains with an odd number of spins and refine previous results for even N in which gaps and spin densities returned slightly different ξ.

The $S = 2$ chain has a smaller Haldane gap [20] of $\Delta(2) = 0.088$. Numerical analysis is more difficult since (i) there are more degrees of freedom per site; (ii) $N > 5\xi$ requires longer chains; and (iii) gaps $\Gamma_S(N) < \Delta(2)$ also require longer chains to distinguish between edge and bulk excitations. Results are fewer and less accurate. The nature of BI-SDWs in $S = 2$ or 3/2 chains was the motivation for DMRG calculations on even and odd chains of hundreds of spins. The spin densities and edge-state gaps of long chains are required to assess theoretical models.

According to the NLσM, edge states for $S = 2$ are associated with spin $s' = S/2 = 1$ in $H_{\rm eff}$, Eq. (4). Even chains have a singlet GS and gaps to two edge states, $\Gamma_1(N)$ to the triplet ($S = 1$) and $\Gamma_2(N)$ to the quintet ($S = 2$). The correlation length ξ is the same for both and $\Gamma_2(N) = 3\Gamma_1(N)$. Neither gap has been reported in chains of more than 200 spins. The VBS valence bond diagram corresponds to two $S = 1$ diagrams in Fig. 1(a): There are four lines per interior $S = 2$ site and two lines, two unpaired spin at the ends. The BI-SDW analysis of $S = 1$ chains is equally applicable to integer S chains. Increasing S leads to longer ξ and to gaps $\Gamma_S(N)$ whose relative magnitudes are fixed in advance by Eq. (4).

A chain with $J = 1$ and 200 spins $S = 2$ or 400 spins $S = 3/2$ has a GS energy of roughly -10^3. The corresponding $\Gamma(N)$ in Table III are less than 10^{-3} and their estimated accuracy is $\pm 1 \times 10^{-4}$. Our $S = 2$ and 3/2 gaps are consequently limited to $N \sim 200$ and 450, respectively. They are differences between total energies. Spin densities, by contrast,

TABLE III. Edge-state energy gaps $\Gamma(N)$, Eq. (2), of HAFs with N spins S and $J = 1$ in Eq. (1).

N	$\Gamma_1(N)$, $S = 2$	$\Gamma_2(N)$, $S = 2$	$\Gamma_1(N)$, $S = 3/2$
64	0.01583	0.05578	0.01276
100	0.00721	0.02452	0.00725
150	0.00255	0.00835	0.00388
200	0.00081	0.00285	0.00268
300			0.00194
400			0.00090
450			0.00065

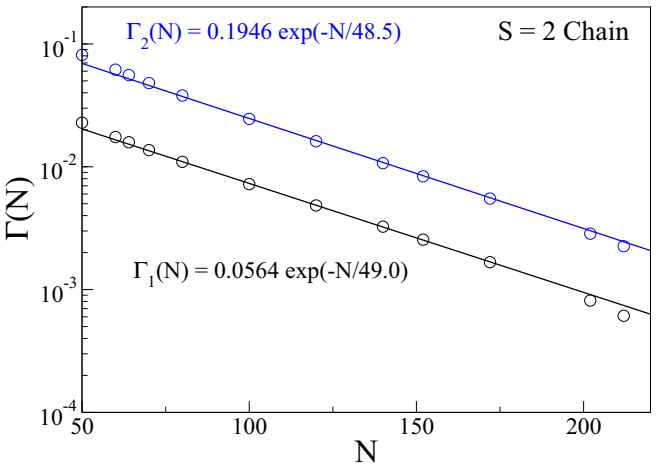

FIG. 4. Edge-state gaps $\Gamma_1(N)$ and $\Gamma_2(N)$ of $S = 2$ chains of N spins in Eq. (1).

are exclusively related to the GS in a sector with $S > 0$. The representative gaps in Table III cover more than a decade. We studied the m dependence of gaps in $S = 2$ and 3/2 chains, summarized in Table I, in order to identify the largest accessible systems. The gap $\Delta(2)$ of the infinite $S = 2$ chain is slightly larger than $\Gamma_2(32)$. The competition between edge and bulk excitations in short HAFs with $S \geqslant 1$ is discussed elsewhere [7–9,22].

Figure 4 shows $\Gamma_1(N)$ and $\Gamma_2(N)$ for $S = 2$ and even N. The gaps are exponential in N/ξ, as expected for integer S. The correlation length, $\xi \sim 49$, is the same within our numerical accuracy. The ratio is $\Gamma_2/\Gamma_1 = 3.45$ based on the fitted lines and it varies between 3.27 and 3.56 for individual points. Although $\Gamma_2/\Gamma_1 = 3.45$ is approximate, the ratio is larger than the NLσM value of 3 based on Eq. (4). We return to gaps after presenting results for spin densities.

$S = 2$ chains with odd N have a quintet GS and excitations to the triplet and singlet. We again use $f(r,N)$ and the BI-SDWs analysis. Figure 5 shows $\ln|f(r,N)|$ in the $S^z = 2$ sector up to the middle of the chains. For the sake of clarity, not all points are shown. Even-odd effects now extend to about the first 25 sites and become size independent in long chains. The thermodynamic limit is $f(r) = \tanh(1/\xi)$ with $\xi = 49.0$. The magnitudes of spin densities in Fig. 6 are fit as a function of r/ξ with the same ξ and $A = 0.90$ in Eq. (7). Two parameters are nearly quantitative aside from sites $r < 25$. The triplet is an excited state for either even or odd N. It is the lowest state in the $S^z = 1$ sector for even N and the first excited state in that sector for odd N. DMRG calculations for even N converge slowly for reasons we do not understand in detail. The triplet spin densities return the same $f(r,N)$ as the quintets in Fig. 5.

The correlation length $\xi = 49.0$ based on spin densities is more accurate than ξ from energy gaps. The $\xi = 49.0$ fits account for $\rho(r,N)$ of even and odd chains that extend to 500 spins, whereas numerical accuracy limits $\Gamma_S(N)$ to $N \sim 200$. Schollwöck *et al.* [6] argued that the thermodynamic limit requires $N > 5\xi$ and obtained (Fig. 6 of [6]) $\xi = 49(1)$ for $N = 270$ with an auxiliary spin-1 at the other end using the local correlation length $\xi(r) = 2/\{\ln[\rho(r-1)/\rho(r+1)]\}$.

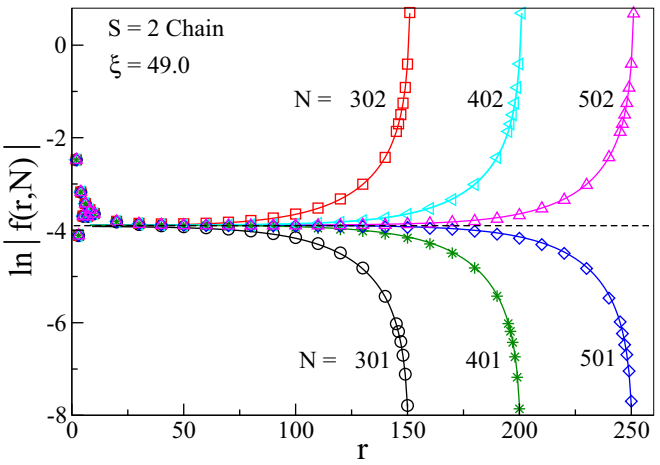

FIG. 5. Open symbols are DMRG spin densities in the $S^z = 2$ sector for $f(r,N)$, Eq. (5), to the middle of $S = 2$ chains of N spins. Solid lines are Eq. (8) with correlation length $\xi = 49.0$. The horizontal dashed line is the thermodynamic limit.

Qin *et al.* [7] estimated that $\xi \sim 33$ for $S = 2$ chains up to $N = 100$ and remarked that the accuracy was much worse than for $S = 1$ chains. Indeed, spin densities for $N = 127$ and 128 return $\xi \sim 36$. As seen in Figs. 3 and 6 for $S = 1$ and 2, respectively, the thermodynamic limit requires $N > 5\xi$ even when the contribution of the BI-SDW at the other end is included. The present results for $S = 2$ chains offer more stringent comparisons of the NLσM. The model is semiquantitative: The ratio $\Gamma_2/\Gamma_1 = 3.45$ is greater than 3. We note that BI-SDWs with exponentially decreasing $|\rho(r,N)|$ would be assumed on general grounds and follow directly from $f(r,N)$. The NLσM accounts for the same ξ for gaps and spin densities.

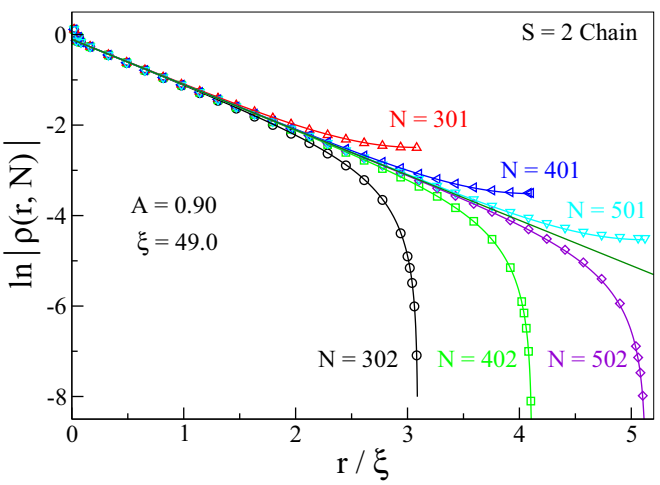

FIG. 6. Open symbols are DMRG results for $|\rho(r,N)|$ in the $S^z = 2$ sector to the middle of $S = 2$ chains. Lines are Eq. (7) with $\xi = 49.0$ and $A = 0.90$. Even and odd N deviate from $A\exp(-r/\xi)$ in the middle.

IV. HALF-INTEGER SPIN, $S = 3/2$

HAF chains with half integer $S \geqslant 3/2$ are gapless and their edge states are fundamentally different. Even chains have a singlet GS and BI-SDWs with integer S; odd chains have $S_G = S$ and BI-SDWs with half integer $S > 1/2$. The even $S = 3/2$ chain has a singlet-triplet gap $\Gamma_1(N)$ that decreases faster than $1/N$ and has been studied by Qin *et al.* [7], and in greater detail by Fáth *et al.* [8]. The NLσM gap goes as [8]

$$N\Gamma_1(N) = \frac{a}{\ln BN} + O\left(\frac{N \ln\ln N}{(\ln N)^2}\right). \tag{9}$$

Fáth *et al.* [8] used DMRG to compute $\Gamma_1(N)$ for $S = 3/2$ chains from $N = 12$ to 192 in steps of 12 spins. The first term of Eq. (9) leads to parameters $a(N)$ and $B(N)$ whose size dependence was obtained from successive gaps $\Gamma_1(N + 12)$ and $\Gamma_1(N)$. Extrapolation in $1/N$ gave the thermodynamic values of $a = 1.58$ and $B = 0.11$ with $\pm 15\%$ uncertainties. In the present study, we are characterizing BI-SDWs in spin chains and take the first term with constant a, B as a two-parameter approximation.

Figure 7 shows the calculated gaps of $S = 3/2$ HAFs as $N|\Gamma(N)|$. The gaps decrease faster than $1/N$ as expected for edge states. The NLσM size dependence for even N is Eq. (4) with $J_e(N) = \Gamma_1 = a/(N \ln BN)$. The dashed line has $a = 1.58$ and $B = 0.11$ as inferred by Fáth *et al.* [8]. The solid line for even N is a power law with two parameters, $\Gamma_1 = J_e(N) = 4.79N^{-1.42}$. Either fit is adequate over this range of system sizes, and neither accounts for the (possible) decrease at $N > 400$. The shortest chains in which edge and bulk excitations are decoupled are probably in the range $N = 30$ to 60, and the desired $\Gamma_1(N)$ fits are for long chains. The gaps $|\Gamma_{3/2}(N)|$ for odd N are several times larger and their size dependence is weaker. They can be approximated by a different logarithm or power law. The gaps $\Gamma_{3/2}(N)$ and $\Gamma_1(N)$ of the $S = 3/2$ chain are in marked contrast to equal $|\Gamma_1(N)|$ in Fig. 1 for $S = 1$ chains with even and odd N.

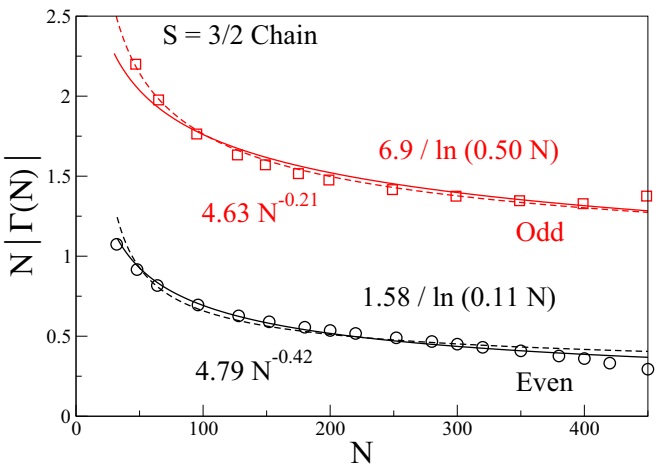

FIG. 7. Open symbols are DMRG results for the gaps $\Gamma_1(N)$ and $|\Gamma_{3/2}(N)|$ for $S = 3/2$ chains with N spins in Eq. (1). The solid and dashed lines are power-law and logarithmic fits, respectively, with two parameters. For even N, the NLσM parameters in Eq. (9) are $a = 1.58$, $B = 0.11$.

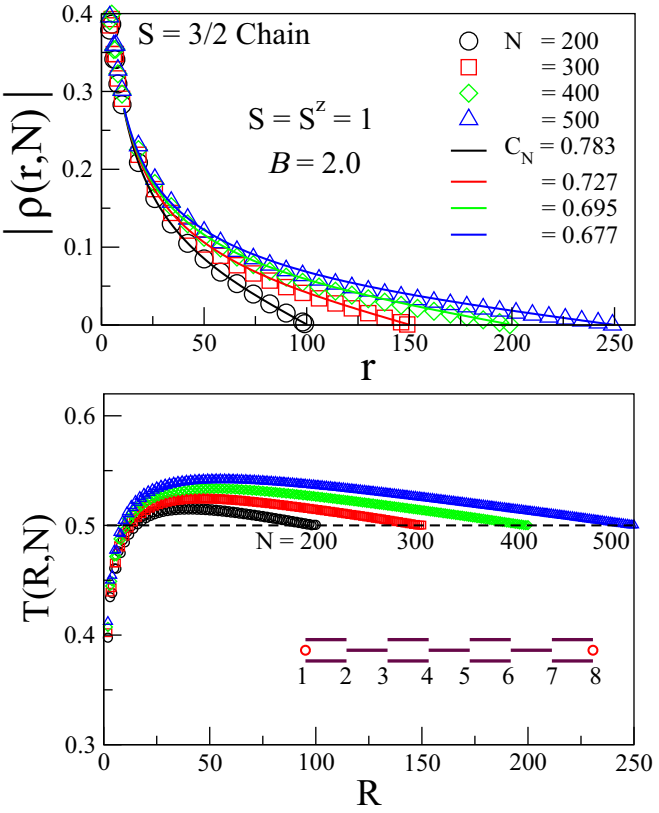

FIG. 8. Upper panel: Open symbols are DMRG spin densities $|\rho(r,N)|$ to the middle of $S = 3/2$ HAFs with even N in Eq. (1). The lines are fits based on Eq. (11) with $B = 2$ and the indicated scale factors C_N. Lower panel: Cumulative spin densities, Eq. (10), up to site R. Inset: VBS valence bond diagram for even N.

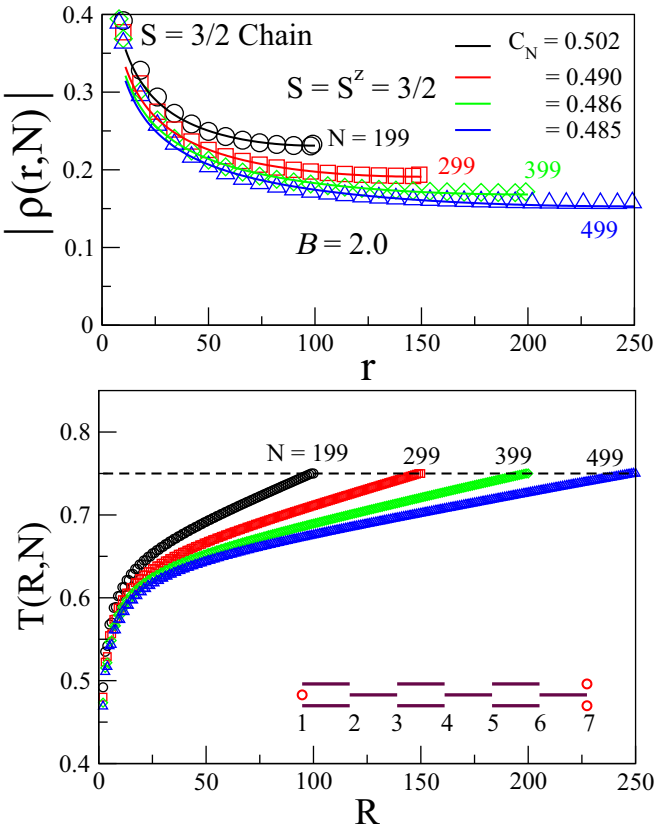

FIG. 9. Upper panel: Open symbols are DMRG spin densities $|\rho(r,N)|$ to the middle of $S = 3/2$ HAFs with odd N in Eq. (1). The lines are fits based on Eq. (11) with $B = 2$ and the indicated scale factors C_N. Lower panel: Cumulative spin densities, Eq. (10), up to site R. Inset: One of two equivalent VBS valence bond diagrams for odd N.

The BI-SDWs of even chains are triplets. The ratios $f(r,N)$ in Eq. (5) are quite different for the $S = 3/2$ chain, either even or odd, and are not shown. The upper panel of Fig. 8 shows the magnitude of spin densities up to the middle of chains. The SDWs converge at small r but are not localized in the $S = 3/2$ chain. The spin densities add up as required to $S^z = 1$ for even N. They decrease slowly and the sum over $|\rho(r,N)|$ diverges in the thermodynamic limit. The lines are fits that are discussed below. The lower panel of Fig. 8 shows the cumulative spin density to site R that we define as

$$T(R,N) = \sum_{r=1}^{R} \rho(r,N) + \rho(R+1,N)/2. \qquad (10)$$

The total spin density is $S^z = 1 = T(N-1,N) + \rho(1,N)/2$. $T(R,N)$ increases rapidly to 0.5 around $R_{1/2} \sim 15$, reaches a broad maximum that depends on system size, and decreases as required by symmetry to 0.5 in the middle of the chain. The VBS valence bond diagram in the inset has unpaired spins at each end that correspond [14] to $s' = (S-1/2)/2 = 1/2$. Each $S = 3/2$ site forms three singlet-paired spins to a neighbor. The middle and either the top or bottom line correspond to the VBS diagram of the $S = 1$ chain with a localized spin at the ends. The remaining line with paired spins is a singlet valence bond diagram of the $S = 1/2$ chain. The slow variation of $T(R,N)$ in the middle and no net spin between $R_{1/2}$ and $N - R_{1/2}$ is consistent with singlet-paired spins.

The GS of odd chains is a quartet, $S = 3/2$. Figure 9, upper panel, shows $|\rho(r,N)|$ to the middle of chains. The large amplitude of in-phase BI-SDWs in the middle decreases slowly with system size. The cumulative spin density $T(R,N)$ in the lower panel is again given by Eq. (10) except that the $r = (N+1)/2$ spin density is shared equally between the two halves. The total is $S^z = 3/2$ for the entire chain, or 0.75 for the half chain. The rapid initial increase to $T(R_{1/2},N) = 0.5$ by $R_{1/2} \sim 15$ suggests a spin-1/2, as does the gradual increase to 0.75 in the middle. The VBS valence bond diagram in the lower panel has three unpaired spins, two at one end and one at the other end; the diagram with reversed unpaired spins at the ends contributes equally by symmetry. The middle and either top or bottom line is again the $S = 1$ VBS diagram. The remaining line is an $S = 1/2$ valence bond diagram with an unpaired spin at either end. Although the diagram correctly has three unpaired spins, the DMRG spin densities clearly show one spin in the central region rather than at the ends.

The $S = 1/2$ HAF with odd N does not support edge states. The spin density is delocalized over the entire chain [23]. Even more simply, a half-filled tight binding or Hückel band of $N = 2n+1$ sites has spin density $1/(n+1)$ at odd numbered sites

and $\rho = 0$ at even numbered sites; in that case, $T(R,N)$ goes as $R/(n+1)$ and immediately rationalizes the linear increase in Fig. 9, lower panel. We attribute the larger gap $|\Gamma_{3/2}(N)| > \Gamma_1(N)$ in Fig. 7 and its weaker dependence of system size to enhanced coupling between the ends by the delocalized spin in the middle.

The BI-SDW amplitude at the middle in the upper panel of Fig. 9 decreases slightly faster than $N^{-1/2}$. The size dependence of the amplitude suggests modeling the spin densities as

$$\rho(r,N) = (-1)^{r-1} C_N \left[\left(\frac{\ln Br}{r} \right)^{1/2} - (-1)^N \left(\frac{\ln B(N+1-r)}{N+1-r} \right)^{1/2} \right]. \quad (11)$$

The amplitude C_N depends on system size because the SDWs are not localized. We took $|\rho(r,N)|$ with $B = 2$ and the indicated C_N to generate the lines in the upper panels of Figs. 8 and 9. The spin densities are adequately fit in the central region in either case. Deviations are seen for $r < 10$ when N is even and for $r < 15$ when N is odd.

To some extent, Eq. (11) can be understood in terms of the NLσM. In the thermodynamic limit, the GS spin correlation functions $C(r)$ depend only on the separation r between spins. The NLσM result is [21]

$$C(r) \equiv \langle S_0^z S_r^z \rangle \propto (-1)^r r^{-1/2} \exp(-r/\xi), \quad (12)$$

for integer spin HAFs and $r \gg \xi$. Several authors [5,21,24] have remarked that DMRG results for $r^{1/2}|C(r)|$ are noticeably closer to exponential in $S = 1$ chains of 60 or 100 spins. Since converged $C(r)$ are limited to about $r < N/4$, such agreement is promising but not forced. White and Huse discuss [5] the point explicitly and show (Fig. 4 of [5]) that the ratio $|C(r)|$ to the NLσM correlation function becomes constant at $r \sim 2\xi \sim 12$. The first few sites where $C(r)$ can be computed the most accurately are inevitably excluded from direct comparison since the NLσM describes a continuous rather than a discrete system. The $r^{-1/2}$ factor in $C(r)$ does not appear in the spin densities of integer S chains [21], whose exponential decrease with r/ξ is shown in Figs. 3 and 6. The spin correlations of the $S = 1/2$ HAF go as $|C(r)| \propto (\ln r/r_0)^{1/2}/r$ according to field theory [13], and Monte Carlo calculations [25] up to $N = 4096$ return $r_0 = 0.08$. But exact results for $C(r)$ in finite PBC systems [25] still show significant deviations at $N = 32$.

Hallberg *et al.* [26] applied the NLσM and DMRG to the $S = 3/2$ chain and confirmed that it belongs to the same universality class as the $S = 1/2$ chain. They report $|C(r)| \propto (\ln Br)^{1/2}/r$ and estimate $B = 0.60$ from $r = 4$ to 25 in a 60-spin chain. We find $B = 0.45$ in similar calculations for $N = 200$. Fáth *et al.* [8] extrapolate to $B = 0.11$ for $\Gamma_1(N)$ in the thermodynamic limit. The differences are negligible in the context of spin densities. Then $r^{1/2}|C(r)|$ gives Eq. (11) when contributions from both ends are taken into account. DMRG results for $|\rho(r,N)|$ deviate from Eq. (11) near the ends of $S = 3/2$ chains and from Eq. (7) in integer S chains. The choice of B changes the fits at small r. Since small r is not modeled quantitatively in either case and does not concern us here, we took $B = 2$ in Eq. (11) for the spin densities of $S = 3/2$ chains.

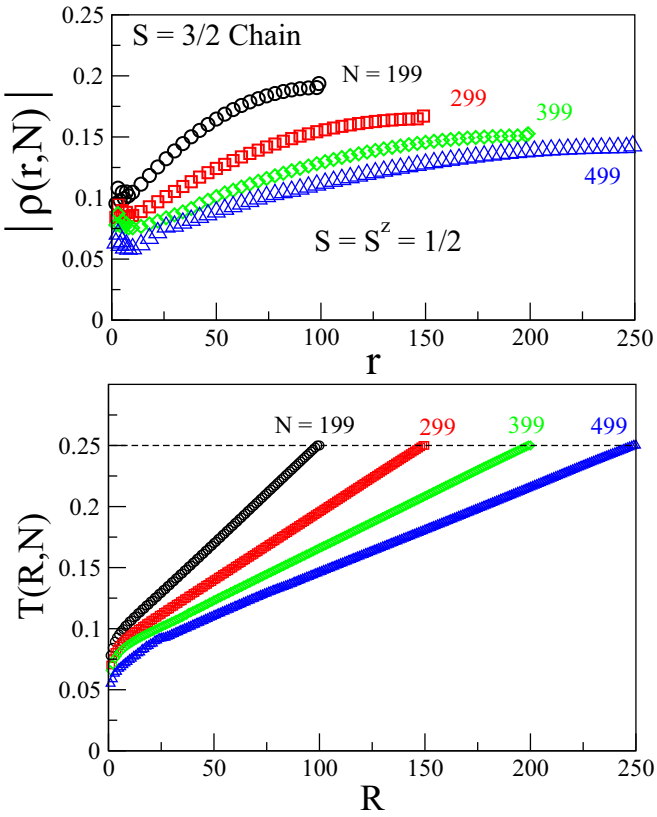

FIG. 10. Upper panel: DMRG spin densities $|\rho(r,N)|$ to the middle of $S = 3/2$ HAFs with odd N in Eq. (1) for the lowest-energy doublet state, $S = S^z = 1/2$. Lower panel: Cumulative spin densities, Eq. (10), up to site R.

Three effective spins are needed for the $S = 3/2$ spin densities when N is odd, a spin s' in the middle in addition to spins at the ends. The generalization of Eq. (4) to half integer S and odd N is

$$H_{\rm eff}(N) = -J_1(N)[\vec{s}' \cdot (\vec{s}'_1 + \vec{s}'_N)] - J_2(N)\vec{s}'_1 \cdot \vec{s}'_N. \quad (13)$$

The eight microstates of $H_{\rm eff}$ correspond to the GS quartet and two doublets. Both the total effective spin S' and $S'_{1N} = s'_1 + s'_N$ are conserved, with $S' = 3/2$, $S'_{1N} = 1$ in the GS. The doublets have $S' = 1/2$ and $S'_{1N} = 0$ or 1. The spectrum is

$$E_{\rm eff}(S', S'_{1N}) = -\frac{J_1}{2} S'(S'+1) + \frac{J_1 - J_2}{2} S'_{1N}(S'_{1N}+1) + \frac{3(J_1 + 2J_2)}{8}. \quad (14)$$

The gap $\Gamma_{3/2} = -J_1/2 - J_2$ is to the doublet with singlet-paired spins at the ends; the gap to parallel spins is $-3J_1/2$. The effective exchanges in Eq. (13) can be fit to DMRG results for the doublets with the lowest and second lowest energy in the $S^z = 1/2$ sector. We find $J_1(99) = 0.04214$, $J_2(99) = -0.00346$ and $J_1(199) = 0.01836$, $J_2(199) = -0.00176$. Large $|\Gamma_{3/2}(N)|$ in Fig. 7 for odd N is due to $J_1(N)$ and coupling through the delocalized effective spin s'. The small effective exchange $J_2(N)$ is ferromagnetic.

To conclude the discussion of $S = 3/2$ chains, we recall that the GS for PBC and odd N has $S_G = 1/2$. Since $J_{1N} = J$ is between sites in the same sublattice, the system is not bipartite, and the GS has a domain wall or topological soliton. The OBC system is bipartite. The doublet $S = S^z = 1/2$ with the lowest energy has positive spin densities at odd-numbered sites and negative spin densities at even-numbered sites, respectively, with singlet paired s'_1 and s'_N in Eq. (13). Figure 10 shows $|\rho(r,N)|$ for $S = S^z = 1/2$ to the middle of $S = 3/2$ chains in the upper panel and the cumulative spin density $T(R,N)$ in the lower panel. The magnitude of the spin density at the middle decreases roughly as $N^{-0.42}$. There are no boundary-induced edge states. The spin is delocalized as expected on general grounds and becomes the effective spin s' in Eq. (13). By contrast, the spin densities are entirely associated with BI-SDWs in OBC systems with even N or integer S since singlet states have $\rho(r,N) = 0$ at all sites.

V. DISCUSSION

We have applied different DMRG algorithms to spin-S HAFs, Eq. (1), with even and odd number sites in order to obtain accurate edge states in chains of several hundred spins. The principal results are the energy gaps $\Gamma_S(N)$, Eq. (2), and the spin densities $\rho(r,N)$, Eq. (3), that are modeled as boundary-induced spin density waves (BI-SDWs) at both ends. For the $S = 1$ HAF, we reproduce and refine previous studies on even chains of 60 or 100 spins that exceed the correlation length $\xi = 6.048$ by an order of magnitude. We confirm that the gap goes as $(-1)^N J_e \exp(-N/\xi)$ in chains with odd N. Two parameters, ξ and the SDW amplitude, account quantitatively for $\Gamma_1(N)$ and $\rho(r,N)$ for chains from $N = 35$ to at least 120. The BI-SDWs are in phase for odd N and out of phase for even N.

The smaller Haldane gap of the $S = 2$ HAF or the gapless $S = 3/2$ HAF requires substantially longer chains, here up to 500 spins, whose edge states have previously been studied in shorter chains $N < 200$. The spin densities of $S = 2$ HAFs between $N = 199$ and 502 are modeled by BI-SDWs with correlation length $\xi = 49.0$ and amplitude $A = 0.90$. There are now two gaps, $\Gamma_1(N)$ and $\Gamma_2(N)$, that decrease exponentially as r/ξ up to the $N \sim 220$ limit of our numerical accuracy. The gap ratio is $\Gamma_2(N)/\Gamma_1(N) = 3.45$. The gap $\Gamma_1(N)$ of the $S = 3/2$ HAF with even N decreases faster than $1/N$, roughly as $N^{-1.42}$ or as $1/\ln(0.11N)$. The gap $\Gamma_{3/2}(N)$ for odd N has larger amplitude and weaker size dependence. The BI-SDWs of the $S = 3/2$ chain have maximum spin density at the ends but are not localized. The $S = 3/2$ spin densities in chains of more than 100 spins have not been previously reported to the best of our knowledge. The $S = 3/2$ ground state for odd N can be modeled as a spin-1/2 at each end and a spin-1/2 in between.

DMRG calculations can be performed on longer chains of $N \sim 1000$ and/or larger S. But the condition $N > 5\xi$ for integer S is increasingly difficult to satisfy for small Haldane gaps $\Delta(S)$ whose rapid decrease has been reported [20] to $S = 5$. Moreover, the gaps will require extraordinary accuracy since, as shown in Table III, $\Gamma(N) < 10^{-3}$ is reached at $N = 200$ for $S = 2$ or at $N = 400$ for $S = 3/2$. Spin densities are more promising probes of long chains in terms of the $S^z > 0$ sectors of N and $N - 1$ spins. But the required system size for half integer S is poorly known and may not have been reached in the present work.

The nonlinear sigma model and valence bond solid have been applied to spin chains, primarily to the $S = 1$ HAF in the thermodynamic limit. Machens *et al.* [9] summarize and critically evaluate both the NLσM and VBS in connection with short chains of less than 20 spins. In partial disagreement with earlier works, they find that the effective coupling between edge states in Eq. (4) in short chains is influenced by the comparably small finite-size gaps of bulk excitations. We have characterized long chains whose prior modeling has mainly been for $S = 1$.

Accurate DMRG results for $S = 2$ or $3/2$ HAFs are a prerequisite for comparisons, mainly via $H_{\rm eff}$ in Eq. (4), with either the NLσM or VBS. Good agreement in $S = 1$ chains carries over to some extent to $S = 2$ chains and less so to $S = 3/2$ chains. Spin densities to $N = 500$ yield $\xi = 49.0$ for the correlation length of the $S = 2$ chain. The gaps in shorter chains return the same ξ, but the ratio $\Gamma_2(N)/\Gamma_1(N)$ is 3.45 instead of 3. The deviation is real.

The $3/2$ chain does not follow the expected [22] $(-1)^N J_e(N)$ pattern of $H_{\rm eff}$ in Eq. (4). The BI-DWIs are not localized. Two effective spins $s' = 1/2$ at the ends account for $\Gamma_1(N)$ when N is even. A third $s' = 1/2$ in the middle leads to $\Gamma_{3/2}(N)$ and the modified $H_{\rm eff}$ in Eq. (13) for odd N.

In other ways, however, comparisons are simply not possible. Since field theory starts with a continuous system rather than a discrete chain, the ends can be distinguished from the bulk but not sites at a finite distance from the ends. Similarly, VBS deals with special Hamiltonians [4,6,9,27] that contain, in addition to Eq. (1), terms that go as $B_p(\mathbf{S}_r \cdot \mathbf{S}_{r+1})^p$ with $2 \leqslant p \leqslant 2S$ and coefficients B_p. Exact GSs are obtained in the thermodynamic limit of these models. The relevant valence bond diagrams have paired spins, as shown, except at the first and last sites. Either the NLσM or VBS correctly places localized states or unpaired spins for integer S, but neither describes the BI-SDWs found in DMRG calculations spin-S HAFs. The BI-SDWs are not localized in half integer S chains and have different effective coupling between ends. Direct solution of Eq. (1) for $S \geqslant 1$ chains inevitably leads to edge states whose features are blurred or lost in the NLσM or VBS. Comparisons may well be limited to effective spins and exchange at the ends.

The occurrence of edge states in HAFs with $S \geqslant 1$ follows directly from Eq. (1), as shown in the Introduction. PBC systems with $J_{1N} = J$ have $S_G = 0$ except for half integer S and odd N, when $S_G = 1/2$. OBC systems with $J_{1N} = 0$ have $S_G = 0$ for even N and $S_G = S$ for odd N. The energy per site in the thermodynamic limit cannot depend on boundary conditions for short-range interactions. Different S_G under OBC and PBC implies edge states, or BI-SDWs, in HAF with $S \geqslant 1$ and gaps $\Gamma_S(N)$ relative to $S_G = 0$ for even N or integer S or to $S_G = 1/2$ for odd N and half integer S. The size dependence and interpretation of gaps or spin densities are standard for integer S. The spin densities and gaps of the $S = 3/2$ chain lead to different BI-SDWs for even and odd N. The NLσM or VBS provides useful guidance for quantitative modeling of BI-SDWs obtained by DMRG for HAFs with $S \geqslant 1$.

ACKNOWLEDGMENTS

We thank S. Ramasesha and D. Huse for discussions and the National Science Foundation (NSF) for partial support of this work through the Princeton MRSEC (Grant No. DMR-0819860). M.K. thanks Department of Science and Technology (DST) for a Ramanujan Fellowship (Grant No. SR/S2/RJN-69/2012) and for funding a computation facility through Grant No. SNB/MK/14-15/137.

[1] H. Bethe, Z. Phys. **71**, 205 (1931); L. Hulthén, Ark. Mat. Astron. Fys. **26A**, No. 11 (1938).
[2] F. D. M. Haldane, Phys. Lett. A **93**, 464 (1983).
[3] S. R. White, Phys. Rev. Lett. **69**, 2863 (1992); Phys. Rev. B **48**, 10345 (1993).
[4] I. Affleck, T. Kennedy, E. H. Lieb, and H. Tasaki, Commun. Math. Phys. **115**, 477 (1988).
[5] S. R. White and D. A. Huse, Phys. Rev. B **48**, 3844 (1993).
[6] U. Schollwöck, O. Golinelli, and T. Jolicœur, Phys. Rev. B **54**, 4038 (1996).
[7] S. Qin, T.-K. Ng, and Z.-B. Su, Phys. Rev. B **52**, 12844 (1995).
[8] G. Fáth, O. Legeza, P. Lajkó, and F. Iglói, Phys. Rev. B **73**, 214447 (2006).
[9] A. Machens, N. P. Konstantinidis, O. Waldmann, I. Schneider, and S. Eggert, Phys. Rev. B **87**, 144409 (2013).
[10] L. Faddeev and L. Takhtajan, Phys. Lett. A **85**, 375 (1981).
[11] I. Affleck, Phys. Rev. Lett. **56**, 746 (1986); **56**, 2763 (1986).
[12] H. J. Schulz, Phys. Rev. B **34**, 6372 (1986).
[13] I. Affleck, D. Gepner, H. J. Schulz, and T. Ziman, J. Phys. A **22**, 511 (1989).
[14] T.-K. Ng, Phys. Rev. B **50**, 555 (1994).
[15] U. Schollwöck, Rev. Mod. Phys. **77**, 259 (2005).
[16] K. A. Hallberg, Adv. Phys. **55**, 477 (2006).
[17] S. R. White, Phys. Rev. B **72**, 180403 (2005).
[18] M. Kumar, A. Parvej, S. Thomas, S. Ramasesha, and Z. G. Soos, Phys. Rev. B **93**, 075107 (2016).
[19] S. Qin, Y.-L. Liu, and L. Yu, Phys. Rev. B **55**, 2721 (1997).
[20] H. Nakano and A. Terai, J. Phys. Soc. Jpn. **78**, 014003 (2009).
[21] E. S. Sørensen and I. Affleck, Phys. Rev. B **49**, 15771 (1994).
[22] J. Lou, S. Qin, T.-K. Ng, and Z. Su, Phys. Rev. B **65**, 104401 (2002).
[23] Z. G. Soos and S. Ramasesha, Phys. Rev. Lett. **51**, 2374 (1983).
[24] K. Nomura, Phys. Rev. B **40**, 2421 (1989).
[25] A. W. Sandvik, in *Lectures on the Physics of Strongly Correlated Systems XIV: Fourteenth Training Course in the Physics of Strongly Correlated Systems*, edited by A. Avella and F. Mancini, AIP Conf. Proc. No. 1297 (AIP, New York, 2010), p. 135.
[26] K. Hallberg, X. Q. G. Wang, P. Horsch, and A. Moreo, Phys. Rev. Lett. **76**, 4955 (1996).
[27] K. Totsuka and M. Suzuki, J. Phys. Condens. Matter **7**, 1639 (1995).